



HAL
open science

Comparative structural analysis of biarylphosphine ligands in arylpalladium bromide and malonate complexes

Anne-Sophie Goutierre, Huu Vinh Trinh, Paolo Larini, Rodolphe Jazzar, Olivier Baudoin

► **To cite this version:**

Anne-Sophie Goutierre, Huu Vinh Trinh, Paolo Larini, Rodolphe Jazzar, Olivier Baudoin. Comparative structural analysis of biarylphosphine ligands in arylpalladium bromide and malonate complexes. *Organometallics*, 2017, 36 (1), pp.129-135. 10.1021/acs.organomet.6b00535 . hal-01484276

HAL Id: hal-01484276

<https://hal.science/hal-01484276v1>

Submitted on 19 Nov 2024

HAL is a multi-disciplinary open access archive for the deposit and dissemination of scientific research documents, whether they are published or not. The documents may come from teaching and research institutions in France or abroad, or from public or private research centers.

L'archive ouverte pluridisciplinaire **HAL**, est destinée au dépôt et à la diffusion de documents scientifiques de niveau recherche, publiés ou non, émanant des établissements d'enseignement et de recherche français ou étrangers, des laboratoires publics ou privés.

Comparative Structural Analysis of Biarylphosphine Ligands in Arylpalladium Bromide and Malonate Complexes

Anne-Sophie Goutierre,[†] Huu Vinh Trinh,[†] Paolo Larini,[†] Rodolphe Jazzar,[†] and Olivier Baudoin^{*,†,‡}

[†]Université Claude Bernard Lyon 1, CNRS UMR 5246 - Institut de Chimie et Biochimie Moléculaires et Supramoléculaires, CPE Lyon, 43 Boulevard du 11 Novembre 1918, 69622 Villeurbanne, France.

[‡]Current address: Department of Chemistry, University of Basel, St. Johanns-Ring 19, CH-4056 Basel, Switzerland.

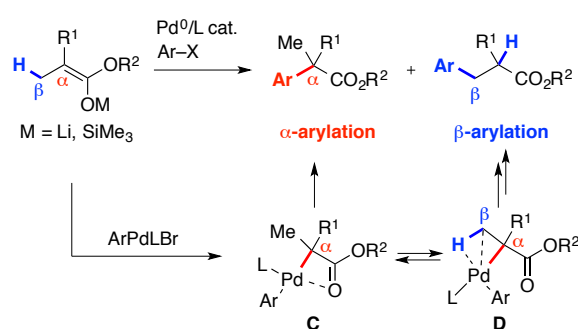
Supporting Information Placeholder

ABSTRACT: The substitution of biarylphosphine ligands was shown to have a marked impact on the α/β selectivity of the arylation of ester enolates. To get further insight into this effect, the solid-state structures of arylpalladium bromide and malonate complexes with four different biarylphosphine ligands were obtained by X-ray diffraction analysis. Structural differences were not very pronounced except for the conformationally restricted CPhos ligand, which showed a bidentate coordination mode in the oxidative addition complex, whereas the other ligands form dimeric species.

INTRODUCTION

The achievement of catalyst-controlled site-selectivity in catalytic transformations is a topic of increasing interest.¹ However, the rational design of selective catalysts is often hampered by a lack of precise information on substrate-catalyst interactions during the selectivity-determining step(s). We have recently developed a Pd-catalyzed migrative arylation of ester enolates^{2a-c} and silyl ketene acetals,^{2d} which allows to functionalize remote C–H bonds of linear alkyl chains of esters. In this process, the arylation selectivity was shown to be both ligand- and substrate-controlled (Scheme 1). In particular, by testing a number of analogous biarylphosphine ligands on the arylation of isobutyric ester enolates ($R^1 = \text{Me}$), we found that the substitution pattern of the former had a great influence on the arylation selectivity.^{2b} Previous studies from Barder and Buchwald demonstrated the effect of binding modes and conformations of biarylphosphine ligands on elementary steps of various cross-coupling reactions.³ Such effects are likely to operate as well in migrative cross-coupling reactions, hence a better understanding thereof should have important implications for the development of new variants.⁴⁻⁵ Herein, we describe a structural study of model biarylphosphine–arylpalladium bromide and malonate complexes, which represents a first step toward this goal.

Scheme 1. α - vs. β -Arylation of Ester Enolates

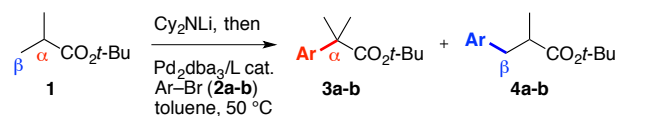


RESULTS AND DISCUSSION

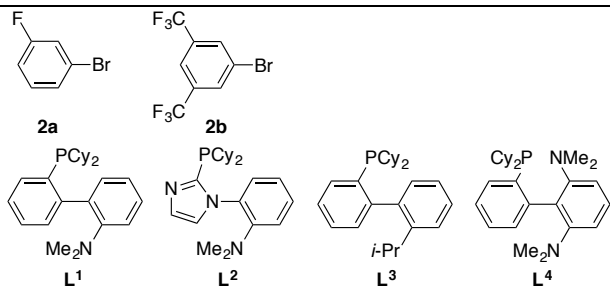
Catalytic reactions with representative biarylphosphines. The effect of four representative biarylphosphine ligands on the selectivity of the arylation of the lithium enolate of *tert*-butylisobutyrate **1** with two different aryl bromides is shown in Table 1. With *m*-fluorobromobenzene **2a** as the electrophile, ligand **L**¹ (DavePhos)⁶ furnished an α/β (**3a/4a**) ratio of 47:53, in line with previous results (entry 1).^{2a-b} A similar ratio was obtained with second generation imidazole-based ligand **L**² (entry 2).^{2c-d} Ligand **L**³,⁷ which is isosteric to **L**¹, significantly altered the α/β ratio in favor of α -arylated product **3a** (entry 3). CPhos **L**⁴, bearing two NMe₂ groups on the non-phosphine-containing ring,⁸ had a dramatic effect on the selectivity, with **3a** being exclusively obtained (entry 4). This is consistent with the fact that this ligand was developed to avoid Pd migration in Negishi-type cross-couplings. The same overall trend was observed with aryl bromide **2b** bearing two strong electron-withdrawing CF₃ groups at the meta positions (entries 5-8). Indeed, ligands **L**¹-**L**² bearing only one NMe₂ group mainly gave β -arylated product **4b** (entries 5-6), whereas ligand **L**⁴ gave **3b** as the major product (entry 8), and ligand **L**³ was somewhat in between (entry 7). However, the impact of the ligand on the arylation selectivity was less pronounced for aryl bromide **2b** compared to **2a**, in line with previous results. This is due to a higher degree of substrate-

controlled selectivity for aryl bromide **2b** containing two strongly electron-withdrawing CF₃ groups. Hence, the nature and number of ortho substituents on the non-phosphine-containing ring of ligands **L**¹-**L**⁴ have a marked effect on the arylation selectivity, thereby pointing to the influence of electronic and/or conformational factors within the Pd intermediates during the reaction. To further investigate these effects, ligands **L**¹-**L**⁴ were chosen for the preparation and study of arylpalladium bromide and malonate complexes.

Table 1. Effect of Representative Biarylphosphine Ligands on the α/β Selectivity of the Arylation of Ester Enolates^a



Entry	ArBr	Ligand	α/β ratio ^b
1	2a	L ¹	47:53
2	2a	L ²	49:51
3	2a	L ³	65:35
4	2a	L ⁴	>99:1
5	2b	L ¹	15:85
6	2b	L ²	17:83
7	2b	L ³	27:73
8	2b	L ⁴	85:15



^a Reaction conditions: **1** (1.6 equiv), Cy₂NLi (1.7 equiv), aryl bromide (1 equiv), Pd₂dba₃ (5 mol%), ligand (10 mol%), toluene, 50 °C. ^b Determined by ¹⁹F NMR.

Synthesis and characterization of oxidative addition complexes containing ligands **L¹-**L**⁴.** Palladium complexes **A**¹-**A**⁴ were prepared in one step by addition of **2b** to a 1:1 mixture of the appropriate ligand and (COD)Pd(CH₂SiMe₃)₂ in THF at 20 °C, and they were isolated as pure solids in reasonable yields (48-86%). Aryl bromide **2b** was chosen after initial investigations with **2a** due to a higher stability of the corresponding bromide and malonate complexes (*vide infra*). Indeed,

the strong electron-withdrawing CF₃ substituents in **2b** should stabilize the corresponding aryl-palladium complexes by strengthening the C_{Ar}-Pd bond.^{2b,9} Suitable monocrystals of **A**¹-**A**³ were readily obtained from a CDCl₃/hexane mixture, and the corresponding X-ray structures are shown in Figure 1. In the solid state, complexes **A**¹-**A**³ display a bromo-bridged dimeric structure (**A**¹_{dim}-**A**³_{dim}), with **A**¹_{dim} having a bent character between the two palladium units along the Br-Br axis (137.2°), presumably to minimize steric repulsions between the respective **L**¹ ligands. In all structures the sum of the angles around the palladium center ranging between 359.6°-361.7° demonstrates planarity at the metal with only minor distortions. In contrast, the X-ray crystallographic analysis of complex **A**⁴ revealed a monomeric species featuring an interaction between the palladium center and the biphenyl *ipso* carbon (C₁₆). The presence of this type of Pd-C_{ipso} bond in palladium(II)-biarylphosphine oxidative addition complexes has been previously reported with CPhos **L**⁴ as the ligand^{8b} and in structurally related BrettPhos-type ligands bearing *i*-Pr instead of NMe₂ groups.¹⁰ The Pd-C_{ipso} bond length of 2.467(3) Å in **A**⁴ lies in the range of distances reported in these CPhos (2.478 Å) and BrettPhos-based complexes (2.439-2.527 Å). As expected, the Pd-C_{ipso} interaction causes a pyramidalization at C₁₆ and an elongation of the C₁₆-C₁₇ and C₁₆-C₂₄ aromatic bonds to 1.431(4) and 1.442(4) Å, respectively. In addition, the C₂₄-N₂₅ bond is significantly shorter (1.383(4) Å) than the other *ortho* C₁₇-N₁₈ bond (1.432(4) Å) and N₂₅ is less pyramidalized than N₁₈ (sum of the bond angles at N₂₅ and N₁₈: 355.0 and 338.6°, respectively), thereby indicating a non-symmetrical participation of these nitrogen atoms to the bonding interaction with Pd.¹¹ In contrast to **A**⁴, complexes **A**¹_{dim}-**A**³_{dim} do not show any real bonding interaction between Pd and the non-phosphine-containing ring of the ligand in the solid state. Indeed, the Pd atom shows no pyramidalization in **A**¹_{dim}-**A**³_{dim}, with its coordination sphere being completed by the μ -bromo ligand, and the shortest distance between Pd and the non-phosphine-containing ring ranges from 3.06 (**A**³_{dim}) to 3.42 Å (**A**¹_{dim}) (Figure 1). In addition, the *ortho* NMe₂ or *i*-Pr group in **A**²_{dim}-**A**³_{dim} is pointing away from the metal, whereas the NMe₂ group is pointing toward Pd in **A**¹_{dim}. It should be also noted that imidazole-based ligand **L**² does not exhibit coordination of Pd by the imidazole nitrogen atom, in contrast to a previous X-ray structure with an analogous ligand.¹²

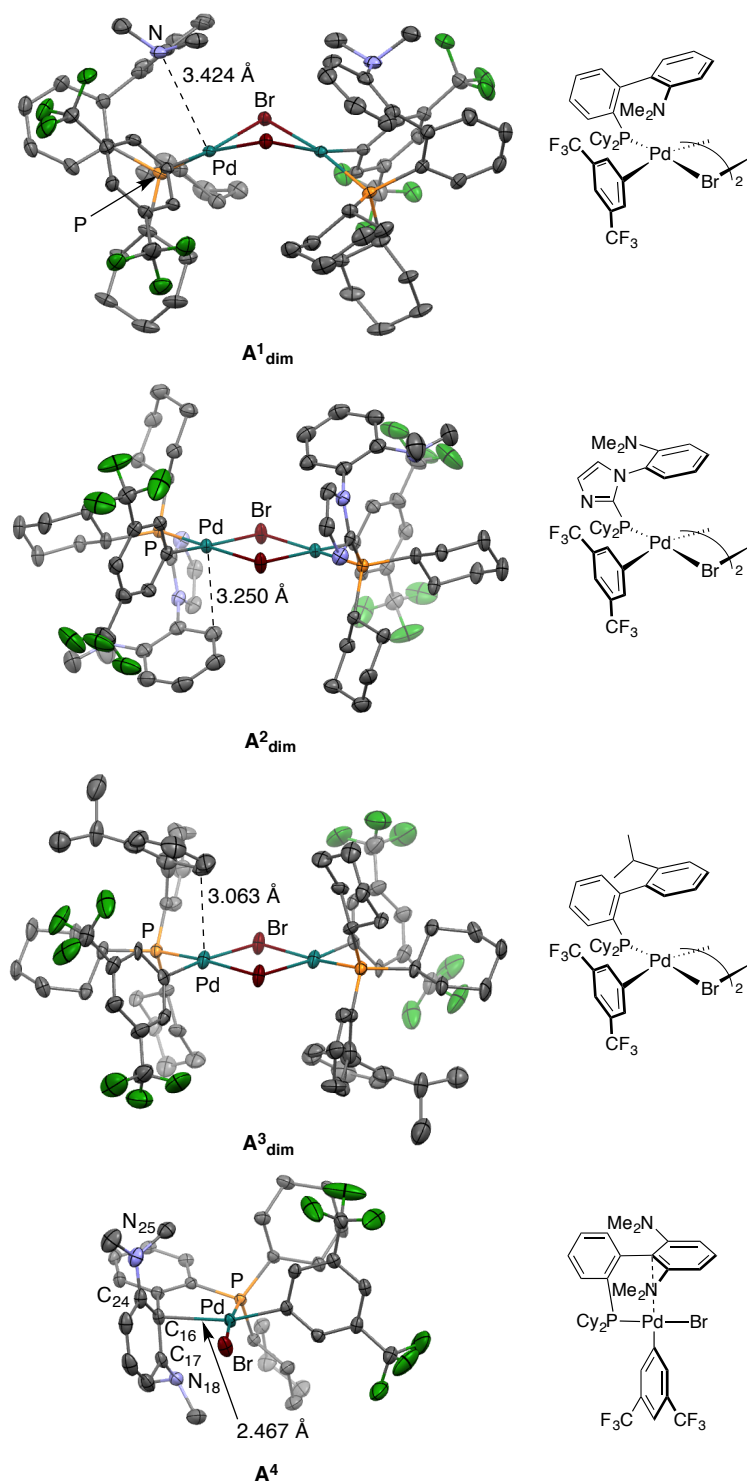


Figure 1. X-ray crystal structures of oxidative addition complexes **A**¹-**A**⁴ showing selected distances (ellipsoids at 50% probability, H atoms omitted for clarity).

Thus, the above structures highlight a significant bonding behavior between ligands **L**¹-**L**³ and **L**⁴. In solution in CDCl₃ at 20 °C, complex **A**¹ mainly occurs as the bromo-bridged dimer **A**¹_{dim}, as indicated by the presence of a sharp singlet resonating at 29.8 ppm in ³¹P{¹H} NMR

(see the Supporting Information). However, in C₆D₆, i. e. in a solvent that has closer properties to the actual solvent employed in catalysis (toluene), the ³¹P{¹H} NMR spectrum of **A**¹ shows a broad signal resonating at 54 ppm, characteristic of a monomeric species. This observation is in accordance with NMR studies by Buchwald, Barder and co-workers.^{3c} Similarly, ³¹P{¹H} NMR analyses indicate that complexes **A**²-**A**³ occur as monomeric species in C₆D₆ and as mixtures of monomer and bromo-bridged dimer in CDCl₃. In contrast, complex **A**⁴ occurs as a single monomeric species in CDCl₃, in agreement with previous data.^{8b} However, its ³¹P{¹H} NMR spectrum in C₆D₆ shows two signals ascribed to two different monomeric species.^{3c} Unfortunately, we were unable to obtain additional information from NMR data due to the fluxional behavior of the above complexes, even by performing variable temperature experiments.

Synthesis and characterization of malonate complexes containing ligands **L**¹-**L**⁴.

On the basis of DFT calculations, we previously proposed that α -arylated products (**3a-b**, Table 1) arise from the reductive elimination of O-bound Pd enolate **C** (Scheme 1).^{2b} On the other hand, the equilibration of **C** to β -agostic complex **D** opens up the β -arylation pathway, which proceeds through β -hydride elimination, rotation, insertion and reductive elimination.^{2b} Culkin and Hartwig showed that the stability of arylpalladium enolate-diphosphine complexes is inversely proportional to the substitution at the α carbon.¹³ In accordance with these results, we were unable to isolate Pd enolates from the reaction of the potassium enolate of **1** with oxidative addition complexes ArPdLBr (L = biarylphosphine). As a consequence, we turned our attention to malonate complexes, as more stable surrogates of Pd enolates **C**-**D**.¹⁴ We initially attempted to prepare such a complex from the oxidative addition complex, obtained from DavePhos **L**¹ and 1-bromo-2-fluorobenzene, that we previously reported.^{2b} Unfortunately in this case, we were not able to isolate the malonate complex, and observed the formation of the α -arylated product. Although it proved difficult to prepare malonate complexes that were sufficiently stable to be isolated and crystallized, we found that the presence of the two electron-withdrawing CF₃ groups on the aryl ligand provided the required stability. Metathetical exchange between the potassium salt of dimethyl malonate (**5a**) and the bromide ligand in com-

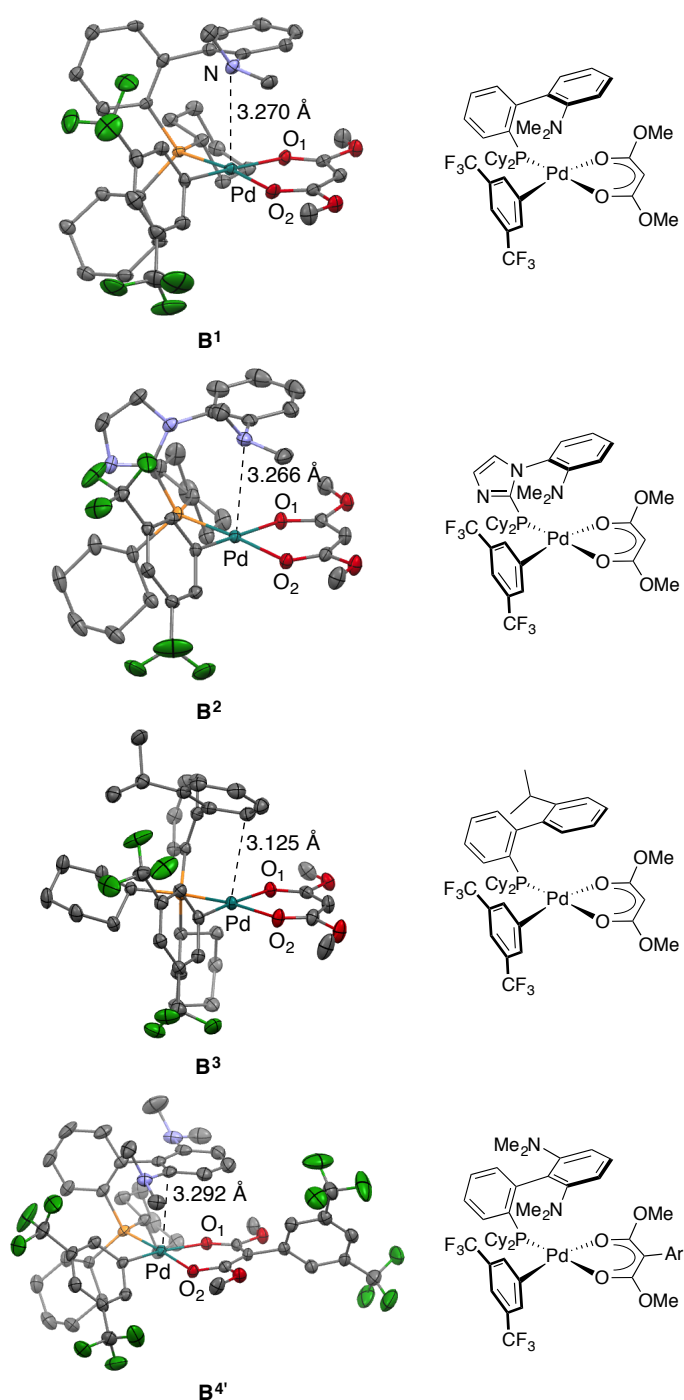


Figure 2. X-ray crystal structures of malonate complexes **B**¹-**B**³ and **B**⁴ showing selected distances (ellipsoids at 50% probability, H atoms omitted for clarity).

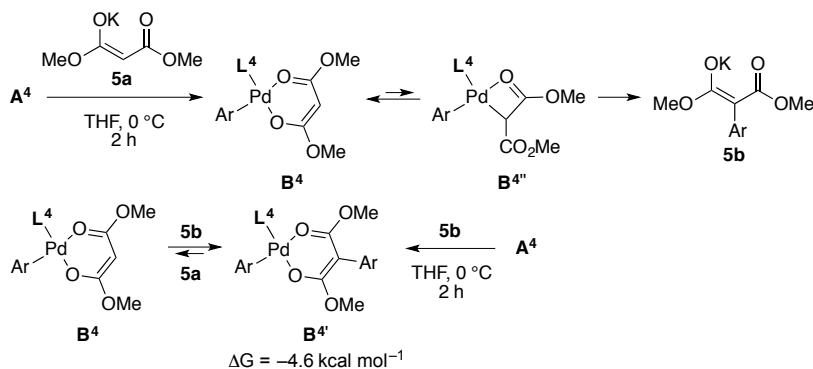
plexes **A**¹-**A**³ readily occurred in THF at 0 °C to generate the κ^2 -O,O'-bound palladium dimethyl malonate complexes **B**¹-**B**³ which could be fully characterized. The X-ray crystal structures of **B**¹-**B**³ are shown in Figure 2. No unusual angles at the palladium center were found in **B**¹-**B**³. As expected, the Pd-O₁ bonds *trans* to the aryl ligand are longer than the Pd-O₂ bonds *trans* to the phosphine ligand (2.107(3) Å vs. 2.091(1) Å for **B**¹; 2.115(1)

Å vs. 2.094(1) Å for **B**²; 2.115(2) Å vs. 2.095(2) Å for **B**³). The spatial orientations of the biaryl moieties of the phosphine ligands observed in **A**¹_{dim}-**A**³_{dim} are preserved in **B**¹ and **B**³, but a rotation of the non-phosphine-containing ring of the ligand is observed in **B**², thus placing the nitrogen atom of the NMe₂ moiety at the pseudo-apical position of the Pd center, similar to **B**¹. The shortest distances between this aromatic ring and Pd in **B**¹-**B**³ ranges from 3.12 to 3.27 Å, with no significant pyramidalization at the Pd center, and thus with no particular bonding character, similar to the corresponding oxidative addition complexes **A**¹_{dim}-**A**³_{dim}.

Finally, malonate complex **B**⁴ was readily obtained from complex **A**⁴ under the same reaction conditions (Scheme 2). However, when **B**⁴ was left to crystallize at 5 °C in a C₆D₆/hexane mixture, we were surprised to obtain the crystal structure of the parent complex **B**^{4'} bearing the arylated malonate. Complex **B**^{4'} displays the same κ^2 -O,O'-coordination mode and overall structure as complexes **B**¹-**B**³ (Figure 2, bottom right). It is probably formed by displacement of the malonate ligand in **B**⁴ by the *in situ*-formed arylated malonate anion **5b**, arising from reductive elimination of the putative C-enolate **B**^{4''}. In addition, **B**^{4'} could be obtained directly from **A**⁴ and malonate anion **5b** in a separate experiment. DFT modeling of the isodesmic reaction between **B**⁴ and **B**^{4'} showed that the formation of **B**^{4'} is thermodynamically favored by 4.6 kcal mol⁻¹, which accounts for the isolation of **B**^{4'} rather than **B**⁴.

Discussion. The above results show that CPhos **L**⁴ behaves differently from the other studied ligands in both oxidative addition, where it adopts a bidentate binding mode, and malonate, where it seems to favor reductive elimination, complexes. This behavior can be inferred to the reduced conformational freedom at the biaryl bond of **L**⁴ compared to **L**¹-**L**³, which should lower the energy barrier of C-C reductive elimination by virtue of steric decompression.¹³⁻¹⁴ This property allows to explain the high α -selectivity selectivity in the arylation of *t*-butyl isobutyrate **1** with this ligand (Table 1). Indeed, the two selectivity-determining steps were shown to be the α -reductive elimination and the olefin insertion with DavePhos **L**¹ as the ligand.^{2b} With a more rigid ligand such as CPhos **L**⁴, α -reductive elimination should become energetically more favorable and Pd migration less favorable, thereby favoring the α -arylated product (**3a-b**). Nevertheless, other factors must be involved, as shown with the selectivity differences observed among ligands **L**¹-**L**³, which form structurally similar oxidative addition and malonate complexes. In particular, the hemilabile character of NMe₂-containing ligands **L**¹-**L**² seems to be an important parameter in

Scheme 2. Formation of Malonate Complex B^{4*} ^a



^a Ar = *m*-(CF₃)₂Ph

comparison with L³, which is isosteric but lacks the nitrogen coordinating group. The current study does not allow to decipher this more subtle effect, and further investigations with more dynamic reaction models³ will be conducted in the future to address this challenging issue.

CONCLUSION

This study represents a first step toward the understanding of the origins of the ligand-induced selectivity in the normal (α) vs. migrative (β) arylation of ester enolates. The solid-state structures of two types of arylpalladium complexes, i. e. oxidative addition and malonate, were solved with four representative biarylphosphine ligands. These data highlight the influence of the ligand rigidity, with CPhos (L⁴) showing higher bidentate character and rigidity compared to ligands L¹-L³ bearing only one *ortho* substituent on the non-phosphine containing benzene ring. This rigidity (or conversely, flexibility) is likely a key factor in the control of the arylation selectivity.

EXPERIMENTAL SECTION

General Considerations. Reactions were performed under an atmosphere of argon with rigorous exclusion of moisture from reagents and glassware using standard techniques. Commercially available reagents were used without further purification unless otherwise stated. All bases, phosphines and palladium sources were stored in a glove box. Anhydrous solvents were obtained by distillation over calcium hydride (*n*-hexane) or sodium / benzophenone (THF, toluene). IR spectra were recorded on an FTIR spectrometer and data are reported in reciprocal centimeters (cm⁻¹). NMR spectra (¹H, ¹³C, ¹⁹F and ³¹P) were recorded on a 300, 400 or 500 spectrometer in CDCl₃ (residual peaks ¹H δ 7.26, ¹³C δ 77.16) or C₆D₆ (residual peaks ¹H δ 7.16, ¹³C δ 128.06). Chemical shifts are reported relative to the chemical shift of the residual solvent for ¹H and ¹³C NMR. ¹⁹F NMR and ³¹P NMR spectra are calibrated with an external reference (CFCl₃, δ 0.0, and H₃PO₄, δ 0.0, respectively) and

recorded with complete proton decoupling. Data are reported as follows: chemical shift in parts per million (ppm), multiplicity (s = singlet, d = doublet, t = triplet, q = quartet, m = multiplet, and br = broad), integration value, coupling constant in Hz if applicable.

General Procedure A for the Synthesis of Oxidative Addition Complexes.

A Schlenk tube was charged with [Pd(COD)(CH₂SiMe₃)₂]¹⁵ (200 mg, 0.52 mmol, 1.0 equiv) and phosphine ligand (0.52 mmol, 1.0 equiv), and the solids were dissolved in THF (20 mL). 1-Bromo-3,5-bis(trifluoromethyl)benzene (0.44 mL, 754.0 mg, 2.58 mmol, 5.0 equiv) was then added to the solution and the reaction mixture was stirred for 16 h at rt. All the volatiles were then removed under vacuum and *n*-hexanes

were added. After filtration by cannula transfer under a positive pressure of argon, the solid was dried under vacuum. Crystallization was achieved using NMR Young tubes with CDCl₃/*n*-hexanes or C₆D₆/*n*-hexanes solvent mixtures.

Complex A¹. Complex A¹ was synthesized according to general procedure A using DavePhos L¹ (204 mg) as the ligand. The title complex was obtained as a grey solid in 86% yield, and was crystallized in CDCl₃/*n*-hexanes. ¹H NMR (400 MHz, CDCl₃, 293 K) δ 0.95-1.15 (m, 4H), 1.42-1.62 (m, 6H), 1.64-1.74 (m, 3H), 1.77-1.83 (m, 2H), 1.88-1.97 (m, 3H), 1.99-2.09 (m, 1H), 2.26-2.35 (m, 1H), 2.59-2.72 (m, 2H), 3.01 (s, 6H), 6.94-7.03 (m, 2H), 7.07-7.11 (m, 1H), 7.13-7.17 (m, 1H), 7.31-7.44 (m, 4H), 7.56-7.62 (m, 1H), 7.64-7.71 (m, 2H). ¹³C NMR (100.6 MHz, CDCl₃, 293 K) δ 25.4 (CH₂), 26.0 (CH₂), 26.4 (CH₂), 26.9-27.5 (m, CH₂), 28.9 (d, *J*_{CP} = 3.6 Hz, CH₂), 30.6 (CH₂), 35.2 (d, *J*_{CP} = 23.9 Hz, CH), 36.3 (d, *J*_{CP} = 29.5 Hz, CH), 44.3 (2CH₃), 117.5 (CH), 118.3 (CH), 120.2 (CH), 123.7 (q, *J*_{CF} = 272.8 Hz, 2C_q), 125.9 (CH), 127.1 (d, *J*_{CP} = 5.7 Hz, CH), 128.4 (d, *J*_{CP} = 35.0 Hz, C_q), 128.6 (q, *J*_{CF} = 31.7 Hz, 2C_q), 129.5 (CH), 131.7 (CH), 132.8 (CH), 135.2 (CH), 136.0 (CH), 138.4 (CH), 141.7 (C_q), 145.5 (C_q), 151.1 (d, *J*_{CP} = 17.7 Hz, C_q), 156.3 (C_q). ³¹P NMR (121.5 MHz, C₆D₆, 293 K) δ 54.0. ¹⁹F NMR (282 MHz, C₆D₆, 293 K) δ -61.7. IR (neat) ν 2931, 2855, 1338, 1270, 1120. HRMS (ESI) *m/z* Calcd for C₃₄H₃₉F₆NPPd ([M-Br]⁺): 712.1767; found: 712.1776.

Complex A². Complex A² was synthesized according to general procedure A using 2-(2-(dicyclohexylphosphino)-1*H*-imidazol-1-yl)-*N,N*-dimethylaniline L² (199 mg) as the ligand. After evaporation of THF, *n*-hexanes were added and the reaction mixture was filtered. After evaporation of the filtrate, the title complex was obtained as a yellow solid in 46% yield, and was crystallized in CDCl₃/*n*-hexanes. ¹H NMR (400 MHz, C₆D₆, 293 K) δ 0.75-0.96 (m, 2H), 1.06-1.16 (m, 4H), 1.20-1.30 (m, 1H), 1.46-1.75 (m, 8H), 1.79-2.13 (m, 4H), 2.16-2.36 (m, 3H), 2.27 (br s, 6H), 6.49 (br s, 1H), 6.83-6.91 (m, 1H), 6.93-7.05 (m, 2H), 7.14-7.23 (m, 3H), 7.48 (s, 1H), 7.72-7.93 (br s, 1H). ¹³C NMR (100.6 MHz, C₆D₆, 293 K) δ 26.4 (4CH₂), 27.6 (2CH₂), 27.8 (4CH₂), 27.9 (2CH₂), 30.6 (br), 31.7 (br), 38.1 (br), 43.9 (2CH₃), 117.3 (CH), 120.3 (CH), 122.5 (CH), 124.6 (q, *J*_{CF}

= 273 Hz, 2C_q), 126.6 (CH), 128.4 (CH), 128.5 (q, ²J_{CF} = 31.8 Hz, 2C_q), 128.7 (C_q), 130.3 (C_q), 130.9 (CH), 131.0 (CH), 131.1 (CH), 137.0 (CH), 150.0 (C_q), 152.7 (C_q). ³¹P NMR (121 MHz, C₆D₆, 293 K) δ 33.8. ¹⁹F NMR (282 MHz, C₆D₆, 293 K) δ -61.7. IR (neat) ν 2937, 2856, 1340, 1272, 1121. HRMS (ESI) *m/z* Calcd for C₃₁H₃₇BrF₆N₃PPdNa ([M+Na]⁺): 804.0745; found: 804.0708.

Complex A³. Complex A³ was synthesized according to general procedure A using dicyclohexyl-(2'-isopropylbiphenyl-2-yl)phosphine L³ (204 mg) as the ligand. The title complex was obtained as a yellow solid in 48% yield, and was crystallized in CDCl₃/*n*-hexanes. ¹H NMR (400 MHz, C₆D₆, 323 K) δ 0.93-1.07 (m, 6H), 1.15-1.33 (m, 6H), 1.37-1.75 (m, 11H), 1.78-2.09 (m, 3H), 2.16-2.50 (m, 2H), 2.56-2.76 (m, 1H), 6.87-7.05 (m, 3H), 7.06-7.14 (m, 1H), 7.17-7.38 (m, 4H), 7.44 (s, 1H), 7.67-7.86 (m, 2H). ¹³C NMR (100.6 MHz, C₆D₆, 293 K) δ 23.2 (CH₃), 23.4 (CH₃), 25.8 (br, CH₂), 26.1-26.4 (br, CH₂), 26.4 (CH), 27.1-27.9 (br, CH₂), 30.2-30.6 (br, CH₂), 30.4 (d, ¹J_{CP} = 4.5 Hz, CH), 31.8 (br s, CH₂), 32.7-33.4 (br, CH₂), 36.8-38.9 (br, CH), 117.2 (br, CH), 124.5 (q, ¹J_{CF} = 272.3 Hz, 2C_q), 125.8 (CH), 126.5 (CH), 126.7 (br, CH), 128.3 (CH), 128.5 (q, ²J_{CF} = 33.4 Hz, 2C_q), 129.2 (CH), 129.4 (d, ¹J_{CP} = 6.4 Hz, CH), 130.7 (d, ¹J_{CP} = 10.9 Hz, CH), 133.8 (CH), 134.4-135.1 (CH), 137.0 (C_q), 137.1 (CH), 139.9 (C_q), 144.4 (C_q), 147.0 (C_q), 153.0 (C_q). ³¹P NMR (202 MHz, C₆D₆, 293 K) δ 44.0. ¹⁹F NMR (376 MHz, C₆D₆, 293 K) δ -61.8. IR (neat) ν 2934, 2857, 1340, 1273, 1123. HRMS (ESI) *m/z* Calcd for C₃₅H₄₀F₆PPd ([M-Br]⁺): 711.1814; found: 711.1798.

Complex A⁴. Complex A⁴ was synthesized according to procedure A using CPhos L⁴ (227 mg) as the ligand. The title complex was obtained as a yellow solid in 70% yield, and was crystallized in C₆D₆/*n*-hexanes. ¹H NMR (400 MHz, CDCl₃, 293 K) δ 0.91-1.03 (m, 2H), 1.07-1.31 (m, 6H), 1.35-1.47 (m, 2H), 1.53-1.63 (m, 2H), 1.63-1.80 (m, 6H), 2.00-2.09 (m, 2H), 2.13-2.26 (m, 2H), 2.62 (s, 12H), 6.86-6.92 (m, 2H), 7.08-7.13 (m, 1H), 7.31-7.37 (m, 2H), 7.43-7.49 (m, 1H), 7.59-7.65 (m, 3H), 7.66-7.71 (m, 1H). ¹³C NMR (100.6 MHz, CDCl₃, 293 K) δ 25.9 (2CH₂), 27.5 (d, ¹J_{CP} = 10.9 Hz, 2CH₂), 27.6 (d, ¹J_{CP} = 11.7 Hz, 2CH₂), 29.4 (2CH₂), 30.2 (2CH₂), 36.9 (d, ¹J_{CP} = 24.3 Hz, 2CH), 45.1 (4CH₃), 112.5 (C_q), 114.9 (2CH), 117.3 (CH), 123.7 (q, ¹J_{CF} = 272.1 Hz, 2C_q), 126.1 (d, ¹J_{CP} = 5.5 Hz, CH), 127.8 (d, ¹J_{CP} = 25.0 Hz, C_q), 128.6 (q, ²J_{CF} = 31.8 Hz, 2C_q), 131.3 (CH), 133.5 (C_q), 133.8 (d, ¹J_{CP} = 12.3 Hz, CH), 134.1 (CH), 135.6 (CH), 136.4 (2CH), 140.8 (C_q), 146.9 (d, ¹J_{CP} = 18.6 Hz, C_q), 157.5 (C_q). ³¹P NMR (162 MHz, CDCl₃, 293 K) δ 33.1. ¹⁹F NMR (376 MHz, CDCl₃, 293 K) δ -62.4. IR (neat) ν 2933, 2855, 1339, 1272, 1123. HRMS (ESI) *m/z* Calcd for C₃₆H₄₄F₆N₂PPd ([M-Br]⁺): 755.2189; found 755.2169.

Synthesis of Potassium Dimethyl Malonate (5a). Potassium dimethyl malonate was formed by the addition of 1 equiv of dimethyl malonate to a suspension of 1 equiv of KH in THF. The reaction mixture was stirred until no more degassing of H₂ was observed. Volatiles were removed

from the resulting solution. The resulting solid was washed with *n*-hexanes and stored in the glovebox at -5°C.

General Procedure B for the Synthesis of Malonate Complexes. A Schlenk flask was charged with potassium dimethyl malonate 5a (3.0 equiv) and THF and cooled to 0 °C. The oxidative addition complex (1.0 equiv) in THF was then added at 0 °C. The reaction mixture was stirred for 2 h at 0 °C. After removing the volatiles under vacuum, toluene was added. The solution was filtered by cannula transfer under a positive pressure of argon. The resulting solution was concentrated, and precipitation was attempted by the addition of *n*-hexanes. When the product did not precipitate, it was directly crystallized in NMR Young tubes with CDCl₃/*n*-hexanes or C₆D₆/*n*-hexanes solvent mixtures.

Complex B¹. Complex B¹ was synthesized according to procedure B from A¹ as the oxidative addition complex. Crystallization was performed in C₆D₆/*n*-hexanes. ¹H NMR (500 MHz, C₆D₆, 293 K) δ 0.63-0.72 (m, 1H), 0.85-1.03 (m, 4H), 1.08-1.19 (m, 1H), 1.22-1.61 (m, 12H), 1.70-1.77 (m, 1H), 1.80-1.93 (m, 2H), 2.10-2.18 (m, 1H), 2.53 (s, 6H), 3.17 (s, 3H), 3.23 (s, 3H), 4.91 (s, 1H), 6.85-6.89 (m, 1H), 6.97-7.04 (m, 2H), 7.06-7.11 (m, 2H), 7.12-7.19 (m, 3H), 7.65 (s, 1H), 7.92 (s, 2H). ¹³C NMR (126 MHz, C₆D₆, 293 K) δ 26.6 (d, ¹J_{CP} = 1.8 Hz, 2CH₂), 27.4 (d, ¹J_{CP} = 9.0 Hz, CH₂), 27.7 (d, ¹J_{CP} = 7.4 Hz, CH₂), 28.1 (d, ¹J_{CP} = 13.9 Hz, CH₂), 28.6 (d, ¹J_{CP} = 16.4 Hz, CH₂), 30.1 (2CH₂), 31.5 (d, ¹J_{CP} = 5.9 Hz, CH₂), 34.0 (CH₂), 34.7 (d, ¹J_{CP} = 20.3 Hz, CH), 39.2 (m, CH), 45.3 (2CH₃), 50.7 (CH₃), 51.1 (CH₃), 66.7 (CH), 117.3 (m, CH), 119.8 (CH), 121.8 (CH), 124.7 (q, ¹J_{CF} = 273.2 Hz, 2C_q), 126.7 (d, ¹J_{CP} = 41.7 Hz, C_q), 127.0 (d, ¹J_{CP} = 7.1 Hz, CH), 127.9 (q, ²J_{CF} = 32.3 Hz, 2C_q), 129.9 (CH), 130.0 (d, ¹J_{CP} = 1.9 Hz, CH), 131.7 (CH), 132.4 (CH), 135.1 (d, ¹J_{CP} = 8.6 Hz, CH), 135.2 (C_q), 136.6 (2CH), 146.7 (d, ¹J_{CP} = 10.1 Hz, C_q), 149.9 (d, ¹J_{CP} = 6.7 Hz, C_q), 153.6 (C_q), 174.5 (C_q), 174.9 (C_q). ³¹P NMR (121 MHz, C₆D₆, 293 K) δ 53.2. ¹⁹F NMR (282 MHz, C₆D₆, 293 K) δ -61.9. IR (neat) ν 2941, 1620, 1498, 1342, 1273, 1120. HRMS (ESI) *m/z* Calcd for C₃₄H₃₉F₆NPPd ([M-malonate]⁺): 712.1767; found: 712.1783.

Complex B². Complex B² was synthesized according to procedure B from A² as the oxidative addition complex. Crystallization was performed in C₆D₆/*n*-hexanes. ¹H NMR (300 MHz, C₆D₆, 293 K) δ 0.69-0.84 (m, 2H), 0.88-1.05 (m, 5H), 1.26-1.37 (m, 3H), 1.39-1.61 (m, 10H), 2.00-2.09 (m, 2H), 2.36 (s, 6H), 3.19 (s, 3H), 3.26 (s, 3H), 4.86 (s, 1H), 6.71-6.78 (m, 2H), 6.86-6.90 (m, 1H), 6.98-7.04 (m, 2H), 7.09-7.13 (m, 1H), 7.65 (br s, 1H), 7.71 (br s, 2H). ¹³C-¹H NMR (100.6 MHz, C₆D₆, 293 K) δ 25.9-28.5 (m, CH₂), 30.9 (br, CH₂), 37.6 (br, CH), 44.1 (2CH₃), 50.8 (CH₃), 51.0 (CH₃), 66.7 (CH), 117.4 (m, CH), 120.2 (CH), 121.5 (CH), 124.6 (q, ¹J_{CF} = 272.8 Hz, 2C_q), 127.3 (CH), 129.5 (d, ¹J_{CP} = 27.5 Hz, C_q), 129.6 (C_q), 130.2 (CH), 130.9 (d, ¹J_{CP} = 10.2 Hz, CH), 131.2 (CH), 132.5 (q, ²J_{CF} = 33.9 Hz, 2C_q), 136.3 (2CH), 148.6 (d, ¹J_{CP} = 5.9 Hz, C_q), 151.1 (C_q), 174.4 (C_q), 174.9 (C_q). ³¹P NMR (121 MHz, C₆D₆, 293 K) δ 30.61. ¹⁹F NMR (282 MHz, C₆D₆, 293 K) δ -61.9. IR (neat) ν 2931, 2854, 1620, 1498, 1342, 1273, 1119. HRMS (ESI) *m/z* Calcd for C₃₁H₃₇F₆N₃PPd ([M-malonate]⁺): 702.1670; found: 702.1664.

Complex B³. Complex B³ was synthesized according to procedure B from A³ as the oxidative addition complex. Crystallization was performed in C₆D₆/*n*-hexanes. ¹H NMR (400 MHz, CDCl₃, 293 K) δ 0.77-0.92 (m, 2H), 0.96-1.29 (m, 5H), 1.07 (d, ³J_{HH} = 6.7 Hz, 3H), 1.19 (d, ³J_{HH} = 6.7 Hz, 3H), 1.34-1.47 (m, 2H), 1.55-1.91 (m, 10H), 1.98-2.13 (m, 2H), 2.19-2.31 (m, 1H), 2.71-2.84 (m, 1H), 3.21 (s, 3H), 3.33 (s, 3H), 4.20 (s, 1H), 7.15-7.21 (m, 1H), 7.28-7.34 (m, 3H), 7.35-7.44 (m, 5H), 7.47-7.52 (m, 1H), 7.54-7.63 (m, 1H). ¹³C NMR (100.6 MHz, CDCl₃, 293 K) δ 22.5 (CH or CH₃), 26.2 (d, J_{CP} = 2.6 Hz, CH₂), 26.8 (CH or CH₃), 27.4 (CH₂), 27.6 (CH₂), 27.7 (CH₂), 27.8 (CH₂), 27.9 (CH₂), 30.2 (CH₂), 30.4 (CH₂), 30.6 (CH or CH₃), 31.5 (br, CH₂), 36.0 (d, ¹J_{CP} = 23.4 Hz, CH), 51.1 (2CH₃), 65.3 (CH), 117.0 (m, CH), 123.9 (q, ¹J_{CF} = 272.8 Hz, 2C_q), 125.2 (CH), 126.0 (d, J_{CP} = 40.4 Hz, C_q), 126.1 (CH), 126.8 (d, J_{CP} = 8.3 Hz, CH), 127.9 (q, ²J_{CF} = 32.3 Hz, 2C_q), 129.1 (CH), 129.5 (d, J_{CP} = 2.2 Hz, CH), 130.3 (CH), 133.3 (CH), 134.0 (d, J_{CP} = 7.9 Hz, CH), 135.5 (2CH), 139.3 (d, J_{CP} = 3.1 Hz, C_q), 145.7 (d, J_{CP} = 8.6 Hz, C_q), 147.1 (C_q), 148.1 (d, J_{CP} = 5.3 Hz, C_q), 173.9 (C_q), 174.3 (C_q). ³¹P NMR (162 MHz, CDCl₃, 293 K) δ 39.9. ¹⁹F NMR (376 MHz, CDCl₃, 293 K) δ -62.5. IR (neat) ν 2935, 2361, 1626, 1502, 1341, 1271, 1129. HRMS (ESI) *m/z* Calcd for C₃₅H₄₀F₆PPd ([M-malonate]⁺): 711.1814; found 711.1785.

Dimethyl 2-(3,5-bis(trifluoromethyl)phenyl)malonate.¹⁶ Under argon, a flame-dried Schlenk tube was charged with CuI (0.05 equiv, 19 mg, 0.1 mmol), 2-phenylphenol (0.1 equiv, 34 mg, 0.0281 mL, 0.2 mmol), and Cs₂CO₃ (1.5 equiv, 977 mg, 3 mmol). Then anhydrous THF (2 mL), 3,5-bis(trifluoromethyl)iodobenzene (1 equiv, 680 mg, 0.356 mL, 2 mmol) and dimethyl malonate (2 equiv, 528 mg, 0.457 mL, 4 mmol) were added. The reaction mixture was stirred at 70 °C for 24 h, and then cooled to room temperature, quenched with a saturated aqueous NH₄Cl solution, and extracted with ethyl acetate. The organic layer was washed with brine and dried over MgSO₄. Filtration through a plug of Celite[®] and concentration on a rotary evaporator afforded the crude product which was purified by silica gel chromatography (elution with cyclohexane/ethyl acetate 4:1). ¹H NMR (300 MHz, CDCl₃, 293 K) δ 3.78 (s, 6H), 4.79 (s, 1H), 7.86 (s, 1H), 7.90 (s, 2H); ¹³C NMR (75 MHz, CDCl₃, 293 K) δ 53.4 (2CH₃), 56.9 (CH), 123.2 (q, ¹J_{CF} = 272 Hz, 2C_q), 122.6 (CH), 130.0 (2CH), 132.0 (q, ²J_{CF} = 33 Hz, 2C_q), 135.1 (C_q), 167.4 (2C_q). ¹⁹F NMR (282 MHz, C₆D₆, 293 K) δ -62.8; IR (neat) ν 1124, 1275, 1741, 2959. HRMS (ESI) *m/z* Calcd for C₁₃H₁₀F₆NaO₄ ([M+Na]⁺): 367.0375; found 367.0368.

Complex B⁴. Complex B⁴ was synthesized according to procedure B from A⁴ as the oxidative addition complex. During the synthesis, all vessels were kept at 0 °C. Crystallization was performed in C₆D₆/*n*-hexanes at 0 °C. For characterization purposes, complex B⁴ was also synthesized according to procedure B from A⁴ as the oxidative addition complex and the potassium salt of dimethyl 2-(3,5-bis(trifluoromethyl)phenyl)malonate (**5b**). ¹H NMR (400 MHz, CDCl₃, 293 K) δ 0.64-0.76 (m, 2H), 1.16 (m, 4H), 1.43-1.56 (m, 4H), 1.59-1.69 (m, 4H), 1.72-1.81 (m, 3H), 1.97-2.09 (m, 3H), 2.16-2.26 (m, 2H), 2.40 (s, 12H), 3.26

(s, 6H), 6.88 (m, 2H), 7.24 (m, 1H), 7.39 (br s, 1H), 7.42-7.47 (m, 1H), 7.48-7.52 (m, 2H), 7.62 (br s, 1H), 7.63 (br s, 2H), 7.77 (br s, 2H), 7.83 (m, 1H). ¹³C NMR (100.6 MHz, CDCl₃, 293 K) δ 26.2 (CH₂), 27.5 (CH₂), 27.6 (CH₂), 27.7 (CH₂), 29.7-30.6 (br, CH₂), 31.8 (CH₂), 35.6-35.9 (br, CH), 46.1 (4CH₃), 51.5 (2CH₃), 80.6 (C_q), 115.4 (2CH), 116.9 (m, CH), 118.7 (m, CH), 123.9 (q, ¹J_{CF} = 272.4 Hz, 2C_q), 124.0 (q, ¹J_{CF} = 272.4 Hz, 2C_q), 126.1 (d, J_{CP} = 9.7 Hz, CH), 126.6 (d, J_{CP} = 41.1 Hz, C_q), 127.6 (q, ²J_{CF} = 32.3 Hz, 2C_q), 128.4 (d, J_{CP} = 2.3 Hz, CH), 129.7 (CH), 130.2 (q, ²J_{CF} = 32.3 Hz, 2C_q), 131.1 (C_q), 132.7 (2CH), 135.7 (d, J_{CP} = 8.8 Hz, CH), 136.5 (2CH), 138.1 (d, J_{CP} = 8.1 Hz, CH), 140.5 (2C_q), 143.1 (d, J_{CP} = 6.7 Hz, C_q), 146.4 (d, J_{CP} = 6.7 Hz, C_q), 154.3 (C_q), 170.9 (2C_q). ³¹P NMR (162 MHz, CDCl₃, 293 K) δ 49.3. ¹⁹F NMR (376 MHz, CDCl₃, 293 K) δ -62.5, -62.6. IR (neat) ν 2937, 1626, 1346, 1273, 1126. HRMS (ESI) *m/z* Calcd for C₄₉H₅₂F₁₂N₂O₄PPd ([M-H]⁺): 1097.2520; found: 1097.2453.

X-ray Structural Analyses. Suitable crystals were selected and mounted on a Gemini kappa-geometry diffractometer (Agilent Technologies UK Ltd) equipped with an Atlas CCD detector and using Mo radiation (λ = 0.7107 Å) except for B³ where Cu radiation (λ = 1.5418 Å) was used. Intensities were collected at 150 K for all compounds but B¹ (100 K) and A¹ (120 K) by means of the CrysAlisPro software.¹⁷ Reflection indexing, unit-cell parameters refinement, Lorentz-polarization correction, peak integration and background determination were carried out with the CrysAlisPro software. An analytical absorption correction was applied using the modeled faces of the crystal.¹⁸ The resulting set of *hkl* was used for structure solution and refinement. The structures were solved by direct methods with SIR97¹⁹ and the least-square refinement on F² was achieved with the CRYSTALS software.²⁰ All non-hydrogen atoms were refined anisotropically. The hydrogen atoms were all located in a difference map, but those attached to carbon atoms were repositioned geometrically. The H atoms were initially refined with soft restraints on the bond lengths and angles to regularize their geometry (C---H in the range 0.93--0.98, N---H in the range 0.86--0.89 and O---H = 0.82 Å) and U_{iso}(H) (in the range 1.2-1.5 times U_{eq} of the parent atom), after which the positions were refined with riding constraints. Complex A³ displayed solvent accessible voids of 102 Å³ in the unit-cell were residual electronic density was present. The contribution of the disordered solvent was removed using the SQUEEZE algorithm.²¹

ASSOCIATED CONTENT

Supporting Information.

NMR spectra and X-ray crystallographic data (CIF) of all complexes, DFT calculations (Scheme 2). This material is available free of charge via the Internet at <http://pubs.acs.org>.

AUTHOR INFORMATION

Corresponding Authors

*E-mail: olivier.baudoin@unibas.ch

Notes

The authors declare no competing financial interest.

ACKNOWLEDGMENT

We thank Ministère de l'Enseignement Supérieur et de la Recherche and Institut Universitaire de France for financial support, Johnson Matthey PLC for a loan of palladium salts, and CCIR-ICBMS (Université Claude Bernard Lyon 1) for the allocation of computational resources. We are also grateful to E. Jeanneau (Centre de Diffraction Henri Longchambon, UCBL) for X-ray diffraction analyses.

REFERENCES

- (1) Mahatthanachai, J.; Dumas, A. M.; Bode, J. W. *Angew. Chem. Int. Ed.* **2012**, *51*, 10954.
- (2) (a) Renaudat, A.; Jean-Gérard, L.; Jazzar, R.; Kefalidis, C. E.; Clot, E.; Baudoin, O. *Angew. Chem. Int. Ed.* **2010**, *49*, 7261. (b) Larini, P.; Kefalidis, C. E.; Jazzar, R.; Renaudat, A.; Clot, E.; Baudoin, O. *Chem.–Eur. J.* **2012**, *18*, 1932. (c) Aspin, S.; Goutierre, A.-S.; Larini, P.; Jazzar, R.; Baudoin, O. *Angew. Chem. Int. Ed.* **2012**, *51*, 10808. (d) Aspin, S.; López-Suárez, L.; Larini, P.; Goutierre, A.-S.; Jazzar, R.; Baudoin, O. *Org. Lett.* **2013**, *15*, 5056.
- (3) (a) Barder, T. E.; Walker, S. D.; Martinelli, J. R.; Buchwald, S. L. *J. Am. Chem. Soc.* **2005**, *127*, 4685. (b) Barder, T. E. *J. Am. Chem. Soc.* **2006**, *128*, 898. (c) Barder, T. E.; Biscoe, M. R.; Buchwald, S. L. *J. Organometallics* **2007**, *26*, 2183. (d) Barder, T. E.; Buchwald, S. L. *J. Am. Chem. Soc.* **2007**, *129*, 12003. (e) Ikawa, T.; Barder, T. E.; Biscoe, M. R.; Buchwald, S. L. *J. Am. Chem. Soc.* **2007**, *129*, 13001.
- (4) (a) Seel, S.; Thaler, T.; Takatsu, K.; Zhang, C.; Zipse, H.; Straub, B. F.; Mayer, P.; Knochel, P. *J. Am. Chem. Soc.* **2011**, *133*, 4774. (b) Millet, A.; Larini, P.; Clot, E.; Baudoin, O. *Chem. Sci.* **2013**, *4*, 2241. (c) Millet, A.; Dailler, D.; Larini, P.; Baudoin, O. *Angew. Chem. Int. Ed.* **2014**, *53*, 2678.
- (5) Reviews on biarylphosphine ligands: (a) Martin, R.; Buchwald, S. L. *Acc. Chem. Res.* **2008**, *41*, 1461. (b) Surry, D. S.; Buchwald, S. L. *Angew. Chem. Int. Ed.* **2008**, *47*, 6338. (c) Surry, D. S.; Buchwald, S. L. *Chem. Sci.* **2011**, *2*, 27.
- (6) Old, D. W.; Wolfe, J. P.; Buchwald, S. L. *J. Am. Chem. Soc.* **1998**, *120*, 9722.
- (7) Wolfe, J. P.; Singer, R. A.; Yang, B. H.; Buchwald, S. L. *J. Am. Chem. Soc.* **1999**, *121*, 9550.
- (8) (a) Han, C.; Buchwald, S. L. *J. Am. Chem. Soc.* **2009**, *131*, 7532. (b) Yang, Y.; Niedermann, K.; Han, C.; Buchwald, S. L. *Org. Lett.* **2014**, *16*, 4638.
- (9) Clot, E.; Mégret, C.; Eisenstein, O.; Perutz, R. N. *J. Am. Chem. Soc.* **2009**, *131*, 7817.
- (10) (a) Fors, B. P.; Watson, D. A.; Biscoe, M. R.; Buchwald, S. L. *J. Am. Chem. Soc.* **2008**, *130*, 13552. (b) Watson, D. A.; Su, M.; Teverovskiy, G.; Zhang, Y.; Garcia-Fortanet, J.; Kinzel, T.; Buchwald, S. L. *Science* **2009**, *325*, 1661. (c) Maimone, T. J.; Milner, P. J.; Kinzel, T.; Zhang, Y.; Takase, M. K.; Buchwald, S. L. *J. Am. Chem. Soc.* **2011**, *133*, 18106. (d) Su, M.; Buchwald, S. L. *Angew. Chem. Int. Ed.* **2012**, *51*, 4710. (e) Milner, P. J.; Maimone, T. J.; Su, M.; Chen, J.; Müller, P.; Buchwald, S. L. *J. Am. Chem. Soc.* **2012**, *134*, 19922.
- (11) (a) Kocovsky, P.; Vyskocil, S.; Cisarova, I.; Sejbal, J.; Tislerova, I.; Smrcina, M.; Lloyd-Jones, G. C.; Stephen, S. C.; Butts, C. P.; Murray, M.; Langer, V. *J. Am. Chem. Soc.* **1999**, *121*, 7714. (b) Faller, J. W.; Sarantopoulos, N. *Organometallics* **2004**, *23*, 2008.
- (12) Torborg, C.; Huang, J.; Schulz, T.; Schäffner, B.; Zapf, A.; Spannenberg, A.; Börner, A.; Beller, M. *Chem.–Eur. J.* **2009**, *15*, 1329.
- (13) Culkin, D. A.; Hartwig, J. F. *J. Am. Chem. Soc.* **2001**, *123*, 5816.
- (14) Wolkowski, J. P.; Hartwig, J. F. *Angew. Chem. Int. Ed.* **2002**, *41*, 4289.
- (15) Pan, Y.; Young, G. B. *J. Organomet. Chem.* **1999**, *577*, 257.
- (16) Hennessy, E. J.; Buchwald, S. L. *Org. Lett.* **2002**, *4*, 269.
- (17) CrysAlisPro, Agilent Technologies, Version 1.171.37.33 (release 27-03-2014 CrysAlis171.NET) (compiled Mar 27 2014,17:12:48).
- (18) Clark, R. C.; Reid, J. S. *Acta Cryst.* **1995**, *A51*, 887.
- (19) Altomare, A.; Burla, M.C.; Camalli, M.; Casciarano, G. L.; Giacovazzo, C.; Guagliardi, A.; Grazia, A.; Moliterni, G.; Polidori, G.; Spagna, R. *J. Appl. Cryst.* **1999**, *32*, 115.
- (20) Betteridge, P. W.; Carruthers, J. R.; Cooper, R. I.; Prout, K.; Watkin, D. J. *J. Appl. Cryst.* **2003**, *36*, 1487.
- (21) Sluis, P. v. d.; Spek, A. L. *Acta Cryst.* **1990**, *A46*, 194.

Table of Contents Graphic:

